



Original Article

The radioresistance of clinically relevant radioresistant cell-derived tumors is determined by the cancer cells themselves, rather than by the surrounding stromal cells



Yoshikazu Kuwahara ^{a,b†}, Kazuo Tomita ^{b†*},
Mehryar Habibi Roudkenar ^{b,c},
Amaneh Mohammadi Roushandeh ^d, Tomoaki Sato ^{b**},
Akihiro Kurimasa ^a

^a Division of Radiation Biology and Medicine, Faculty of Medicine, Tohoku Medical and Pharmaceutical University, Miyagi, Japan

^b Department of Applied Pharmacology, Graduate School of Medical and Dental Sciences, Kagoshima University, Kagoshima, Japan

^c Burn and Regenerative Medicine Research Center, Velayat Hospital, School of Medicine, Guilan University of Medical Sciences, Rasht, Iran

^d Department of Anatomy, School of Biomedical Sciences, Medicine & Health, The University of New South Wales, Sydney, Australia

Received 20 June 2025; Final revision received 30 June 2025

Available online 15 July 2025

KEYWORDS

Heterografts;
Mouth neoplasms;
Radiotherapy;
Stromal cells

Abstract *Background/purpose:* We established clinically relevant radioresistant (CRR) cell lines, which proliferate after exposure to 2 Gy/day of X-rays with the same genomic background as the parental cell lines from SAS cells, a cell line derived from oral squamous cell carcinoma. In this study, we tried to analyze whether the radioresistance of the tumor is defined by the stromal cells or the cancer cells using the CRR cells.

Materials and methods: We transplanted parental and CRR cells into nude mice. The effects of 2 Gy/day fractionated radiation (FR) on the tumors were observed for 30 days. We measured tumor size, nuclear size by Hematoxylin-Eosin staining, Ki-67 expression via immunostaining, and Autophagosome formation using Electron microscopy.

* Corresponding author. Department of Applied Pharmacology, Graduate School of Medical and Dental Sciences, Kagoshima University, 8-35-1 Sakuragaoka, Kagoshima 890-8544, Japan.

** Corresponding author. Department of Applied Pharmacology, Graduate School of Medical and Dental Sciences, Kagoshima University, 8-35-1 Sakuragaoka, Kagoshima 890-8544, Japan.

E-mail addresses: ktomita@dent.kagoshima-u.ac.jp (K. Tomita), tomsato@dent.kagoshima-u.ac.jp (T. Sato).

† These authors contributed equally to this work and share first authorship.

Results: From the 20th day of FR, the SAS tumor volume gradually decreased. At 30 days of FR, the SAS tumor volume was reduced by half. Conversely, SAS-R tumors maintained a constant level after FR. The histology of the SAS tumor exhibited advanced fibrosis and enlarged cell nuclei. However, the SAS-R tumor showed no notable fibrosis, and the cell nuclei in the SAS-R tumors were like the nonirradiated cells. The number of Ki-67 positive cells was reduced in SAS tumors but not SAS-R tumors. Electron microscopy revealed autophagosome-like structures in the parent cells, but not in the SAS-R cells.

Conclusion: The cancer cells themselves define the radioresistance of the tumor rather than by the surrounding stromal cells.

© 2026 Association for Dental Sciences of the Republic of China. Publishing services by Elsevier B.V. This is an open access article under the CC BY-NC-ND license (<http://creativecommons.org/licenses/by-nc-nd/4.0/>).

Introduction

Oral cancer is the most common cancer in men in India and Pakistan, and the 16th most common cancer worldwide (2 % of all cancers).¹ In oral cancer, surgery is indicated in the early stages, but 74 % of all head and neck cancer patients are candidates for radiotherapy at some point during their disease course. Radiotherapy may be preferred in oral cancer over surgery to preserve oral function.² Therefore, improving the efficiency of radiotherapy for oral cancer is a significant step toward overcoming these challenges.

In general, radiotherapy is a highly effective anticancer therapy implemented in approximately 50 %–60 % of patients.³ Conventional fractionated radiation (FR) therapy typically delivers doses of 1.8–2 Gy per day, 5 days a week, to eliminate cancer cells while minimizing the harm to healthy tissues. Standard treatment period is of 6–7 weeks, so the total dose is approximately 54–60 Gy. However, some cancer cells develop radioresistance, leading to radiotherapy failure. For example, fractionated radiation has been demonstrated to enhance the radioresistance of certain cancer cells, such as prostate cancer cells.⁴ Hence the presence of radioresistant cells is one of the major obstacles in radiotherapy, and multiple studies have been conducted to address such radioresistant cells.^{5,6}

Comparative analysis of cell lines with different genomic backgrounds and radioresistance have been conducted.^{7,8} We speculated that a comparative approach using cells with different genomic backgrounds can detect factors not involved in radioresistance. Therefore, we established clinically relevant radioresistant (CRR) cell lines with the same genomic background as the parental cell lines.⁹ CRR cells continue to proliferate after exposure to 2 Gy/day of X-rays for more than 30 consecutive days, the standard protocol for tumor radiotherapy. After we established CRR cells, isogenic models of radioresistance have been widely analyzed.^{10–14} These radioresistant cell lines reduce the genetic variations present in patient samples and cell lines of different origins, allowing the identification of molecular determinants of radio response.¹⁵

The radioresistance of cancer cells is influenced by external and internal factors.¹⁶ External factors include the tumor microenvironment and radiation exposure, and internal factors include genetic and molecular characteristics of the cancer cells themselves.¹⁷ It has been reported that

stromal cells in the tumor microenvironment have a significant effect on the radioresistance of cancer cells.^{18,19}

These studies underscore the complexity of the tumor microenvironment and the need to consider stromal cells when developing radiotherapy strategies. On the other hand, it has been reported that radiation-induced stromal cell damage does not significantly contribute to tumor cell death.²⁰ Gerweck et al. and Ogawa et al. showed that the intrinsic radioresistance of tumor cells is a major determinant of tumor response to radiation.^{21,22} Thus, radiation-induced stromal cell damage is not the primary factor in tumor cell death but may play a role in modulating the response to radiotherapy. The role of radiation-induced stromal cell damage in tumor cell death remains controversial and the subject of ongoing research.

The doses of radiation used to study the roles of tumor cells and stroma cells differ from the doses used in radiotherapy. Thus, to investigate the contribution of stroma cells to tumor radioresistance, experiments using the same radiation doses as radiation therapy are needed. We established radioresistant cells that continue to proliferate after exposure to 2 Gy/day X-rays for more than 30 days *in vitro*. In this study, we transplanted CRR cells into nude mice to analyze whether the radioresistance of the tumor was defined by the stromal cells or the cancer cells.

Materials and methods

Cell culture and irradiation

Human oral squamous cell carcinoma cell line (SAS) was obtained from the Cell Resource Center for Biomedical Research, Institute of Development, Aging, and Cancer. SAS CRR (SAS-R) cell line was established by gradually exposing SAS cells to increasing doses of X-rays, as previously described.⁹ Cells were maintained in Roswell Park Memorial Institute 1640 medium (Nacalai Tesque Inc., Kyoto, Japan) supplemented with 5 % fetal bovine serum (Gibco Invitrogen Corp., Carlsbad, CA, USA) in a humidified atmosphere at 37 °C with 5 % CO₂. To maintain the CRR phenotype, SAS-R cells were exposed to 2 Gy of X-rays every 24 h. X-ray irradiation was performed at the dose of 1 Gy/min in a 150-KVp X-ray generator (MBR-1520R; Hitachi Power Solutions Co. Ltd, Tokyo, Japan) with a total filtration of 0.5 mm aluminum and 0.1 mm copper.

Effects of fractionated radiation on xenograft tumors

Male 4-week-old BALB/c nude mice were used for all experiments. All experimental protocols were approved by the Committee on the Ethics of Animal Experiments, Tohoku University, and were conducted according to the University's Guidelines for Animal Experiments. Exponentially growing cells (1×10^7 cells in 250 μL saline) were subcutaneously injected into the backs of the nude mice. Experiments started (day 0) when tumor volumes reached about 250 mm^3 . FR were exposed to mice every 24 h for 30 days. The mice except for the tumor regions, were protected from radiation by a lead shield. Tumor volumes were estimated using a caliper and calculated according to the following formula: tumor volume = $0.5 \times \text{length} \times \text{width} \times \text{height}$.²³

Histological analysis and immunohistochemistry of SAS and SAS-R tumors

Mice with tumors were perfused with 4 % paraformaldehyde (PFA) via the left ventricle of the heart 24 h after the last treatment. The excised tumor tissues were postfixed in 10 % neutral-buffered formalin overnight, and 4- μm thick paraffin-embedded sections were prepared. Sections were stained with hematoxylin and eosin (HE). Cell nucleus size was measured using NIH Image (ImageJ). At least 200 cells per field were counted in tumors from three mice per group.

Tissue sections were heated in antigen retrieval solution (pH 9.0; Nacalai Tesque Inc.) by microwaving for 10 min and cooled to room temperature. After washing twice with phosphate-buffered-saline (PBS), the slides were treated

with 3 % H_2O_2 -methanol for 10 min at room temperature to quench endogenous peroxidase activity. After incubating with 5 % skim milk in PBST for 60 min at room temperature in a humidity chamber to reduce nonspecific staining, the sections were incubated overnight at 4 °C with primary antibodies to detect Ki-67 (sc-15402; Santa Cruz Biotechnology Inc., Dallas, TX, USA; 1:1000 dilution). After washing three times with PBS, the specimens were incubated for 60 min at room temperature with the goat anti-rabbit immunoglobulin (IgG) antibody (H1202; Nichirei Biosciences Inc., Tokyo, Japan; 1:1000 dilution). The signals were visualized with 3,3'-diaminobenzidine followed by counterstaining with HE. Sections were photographed with a BZ-Analyzer (Keyence, Osaka, Japan).

Transmission electron microscopy (TEM)

Tumor tissues were fixed with a mixture of 0.04 % glutaraldehyde and 4.0 % paraformaldehyde in 0.1M phosphate-buffer, pH 7.4 (PB), at 4 °C for 1 h. After cutting into small blocks (approximately 1 mm^3), the tissues were immersed in 2 % glutaraldehyde in 0.1 M PB for 2 h. After washing with Dulbecco's PBS to remove the fixative, the tissue was cut with a razor blade into pieces and post-fixed with 2 % buffered OsO_4 . Tissues were stained *en bloc* in aqueous uranyl acetate solution, dehydrated through a graded series of ethanol solutions and embedded in EPON 812 resin (TAAB Laboratories Equipment Ltd, Aldermaston, UK). Ultrathin resin tissue sections (70 nm) were mounted on copper, counterstained with uranyl acetate and Reynold's lead citrate solution, and then observed with a Hitachi H-9000 electron microscope.

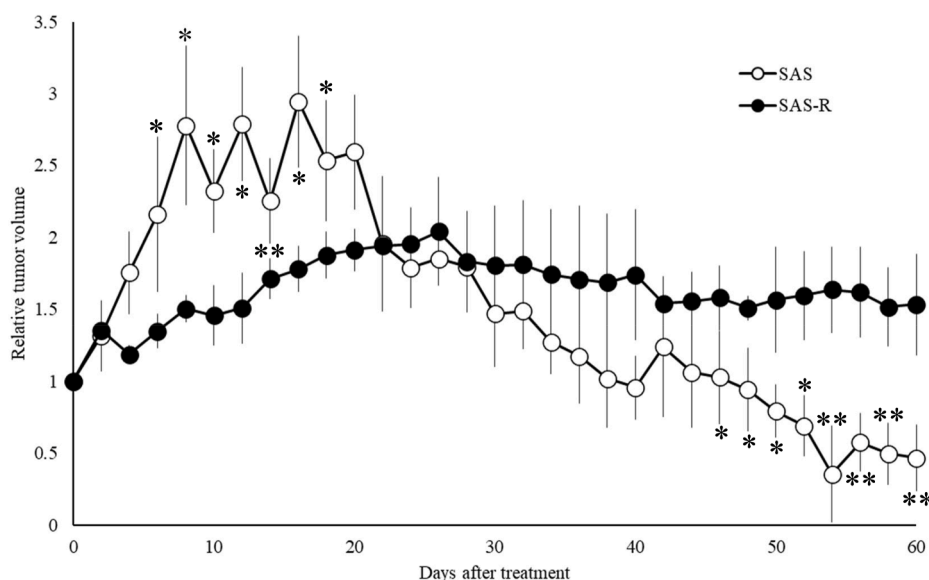


Figure 1 Clinically relevant radioresistant (CRR) tumor model. The left and right backs of the nude mice were subcutaneously injected with exponentially growing parental human oral squamous cell carcinoma cell line (SAS) and SAS CRR (SAS-R) cells, respectively. When tumors reached about 250 mm^3 (day 0), mice were exposed to fractionated radiation at 2 Gy/day of X-rays for 30 consecutive days. The nontumor area was shielded with a lead plate. The vertical axis represents the relative tumor size, and the horizontal axis represents the number of days of treatment. The SAS tumor volume was less than half the beginning volume after 60 days after treatment. In contrast, the volume of SAS-R tumors continued to increase and maintain a constant level. Mean \pm SD of three independent mice is shown. ** $P < 0.01$, * $P < 0.05$.

Statistical analysis

The data were analyzed by Student's *t*-test. A significance level of $P < 0.05$ was adopted. Results are expressed as mean \pm standard deviation (SD) of three independent experiments.

Results

CRR cells exhibit resistance to fractionated X-ray irradiation *in vivo*

For the radiosensitive/radioresistant xenograft mouse model, the left and right backs of the nude mice were subcutaneously inoculated with SAS and SAS-R cells, respectively. After reaching 250 mm^3 , the tumors were irradiated with 2 Gy/day fractionated X-rays per day while shielding the

non-tumor area with a lead plate. SAS tumors continued to grow until 10 days after starting FR (total dose 20 Gy; Fig. 1) to about three times the initial volume. Thereafter, the tumor volume remained approximately the same. The tumor volume gradually decreased from the 20th day of FR. Sixty days after treatment, the SAS tumor volume was less than half the beginning volume. In contrast, the volume of SAS-R tumors continued to increase and maintain a constant level after irradiation with FR at 2 Gy/day. These results demonstrate that the CRR cell xenograft model is useful for the *in vivo* analysis of human radioresistant cells.

Histological analysis of SAS and SAS-R tumors

Histological analysis revealed no differences in tissue structure between SAS and SAS-R tumors before FR (Fig. 2). The nuclei of SAS cells were significantly enlarged after irradiation with 20 Gy (10 FR) compared with the nuclei of

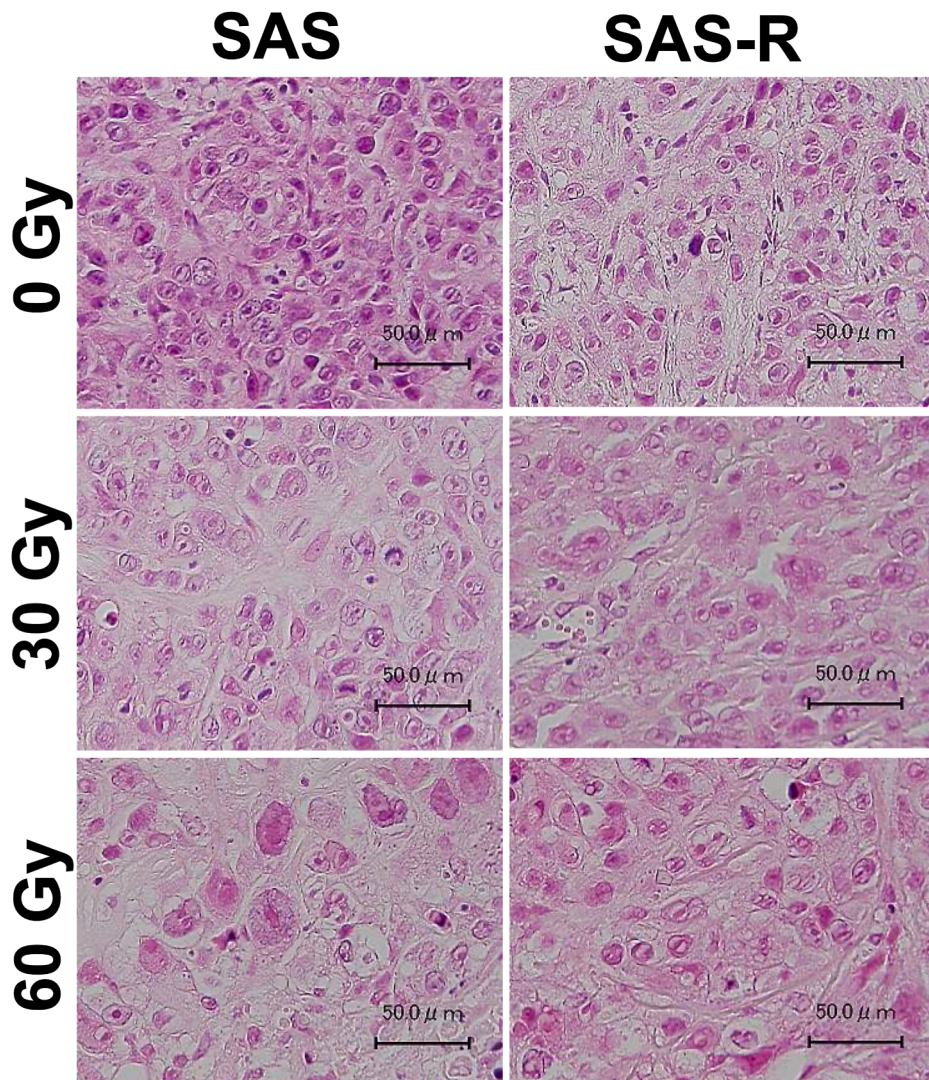


Figure 2 Histology of clinically relevant radioresistant (CRR) tumors. Parental SAS and SAS CRR (SAS-R) tumor tissues irradiated with 0, 30, and 60 Gy of X-rays were fixed in 10 % neutral buffered formalin and 4- μm -thick paraffin-embedded sections were prepared. The sections were stained with hematoxylin and eosin, and the nuclear size of each section were measured. The nuclei of SAS cells were enlarged as the total radiation dose increased, but the nuclei of SAS-R cells did not increase in size.

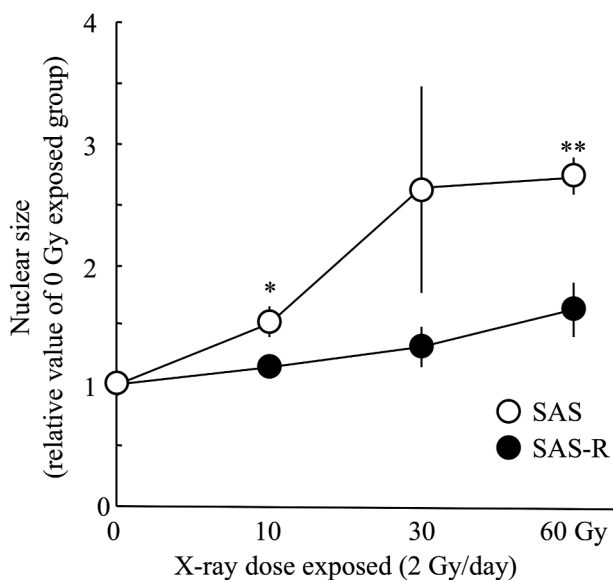


Figure 3 Quantitative analysis of nuclear size. The vertical axis indicates the size of the nucleus, and the horizontal axis indicates the X-ray exposure dose. In SAS tumor cells, as the total radiation dose increased, the size of the nuclei significantly increased. However, the size of nuclei did not increase significantly in response to radiation in SAS-R tumor cells. ** $P < 0.01$, * $P < 0.05$.

SAS-R cells. The nuclei of SAS cells were enlarged about 3-fold compared with non-irradiated nuclei (Fig. 3). Conversely, the nuclei of SAS-R cells were not enlarged after irradiation. These results suggest that SAS-R cells are less affected by FR than SAS cells. Tumor fibrosis of in the stromal cells progressed in both SAS and SAS-R tumors, indicating that stromal cells in SAS and SAS-R tumors were affected by FR. Overall, the histological analyses indicates that the radioresistance of tumors depends on the radioresistance of the tumor cells rather than the tumor stromal cells.

Determining the growth fraction of SAS and SAS-R cell populations

Ki-67 staining was used to determine if tumor cells were proliferatively active when exposed to FR. Many Ki-67-positive cells were observed in both the SAS and SAS-R tumors before irradiation (Fig. 4). After 15 days of FR, no significant differences in the number of Ki-67 positive cells were observed between the SAS and SAS-R tumors. After 30 days of FR, the number of Ki-67 positive cells was reduced in SAS tumors but not SAS-R tumors. Notably, connective tissue increased in the SAS tumors.

Electron microscopic analysis

Electron microscopy revealed no significant differences in SAS and SAS-R tumors before FR (Fig. 5). After irradiation with 30 Gy, numerous double-membraned autophagosome-like vesicles were observed in the cytoplasm in SAS tumors. These vesicles increased in the cytoplasm after exposure to 60 Gy irradiation in the SAS tumors but not the SAS-R

tumors. A small number of autophagosome-like structures were consistently observed in the cytoplasm of SAS-R cells. These observations suggest that fractionated irradiation induces autophagic cell death in SAS cells.

Discussion

Xenograft mouse models are often used as preclinical cancer models to study the clinical behavior and therapeutic progress of radioresistant cancer cells.²⁴ These models allow researchers to observe the interactions between cancer cells and the tumor microenvironment, evaluate the efficacy of various treatments, and elucidate the mechanisms of radioresistance. Thus, these models help bridge the gap between *in vitro* studies and clinical applications. For example, Pan et al. developed radioresistant lung squamous cell carcinoma (LUSC) cell lines, and *in vivo* nude mouse xenograft experiments were conducted to verify the feasibility of these cell lines.²⁵ Zhang et al. detected elevated expression of Rab25, a receptor recycling protein, in an array of radioresistant human cancer cell lines and *in vivo* radioresistant xenograft tumors.²⁶ Xie et al. investigated radioresistant and radiosensitive cancer cell interactions using a radioresistant/radiosensitive xenograft mouse model.²⁷ Thus, the xenograft tumor model is widely used to identify factors contributing to cancer cell radioresistance. However, the X-ray irradiation conditions used in these studies differ from the 2 Gy/day irradiation conditions used in clinical practice. Tumors derived from CRR cells can survive even under irradiation conditions of 2 Gy/day, making this an optimal model for studying radioresistant tumors.

We conducted *in vivo* experiments using CRR cells resistant to 2 Gy/day X-rays, the standard protocol for tumor radiotherapy. After 10 days of FR, tumors derived from SAS cells began to shrink, whereas the size of tumors derived from SAS-R was constant, indicating that the radioresistance of tumors depends on the radioresistance of the tumor cells. The growth rate of SAS-R tumors was slower compared to the growth rate of SAS tumors. Moreover, our previous analysis showed that the doubling time of SAS-R cells was longer than the doubling time of SAS cells; this characteristic may have affected the tumor growth rate.²⁸ We have previously observed the growth of non-irradiated SAS and SAS-R after cell transplantation and confirmed that the tumor size increased over time after transplantation.²⁹ Furthermore, our previous observation showed the same results after irradiation; when SAS was transplanted, the tumor size decreased from 30 days after irradiation, while the tumor size of SAS-R did not increase significantly and remained constant.²⁹ The nuclei of SAS cells but not SAS-R cells were enlarged after FR. Rene et al. detected dose-dependent increased cell size after γ -ray irradiation.³⁰ Increased cell size after radiation treatment was also reported.³¹ Our previous study also demonstrated that the nuclei of the parental HepG2 cells but not CRR HepG2-8960-R cells were enlarged after X-ray irradiation.⁹ Radiation fibrosis is characterized by the development of scar tissue in irradiated tissues and is a late side effect of radiotherapy. Fibrosis is caused by the accumulation of collagen and integrins in the extracellular matrix due to

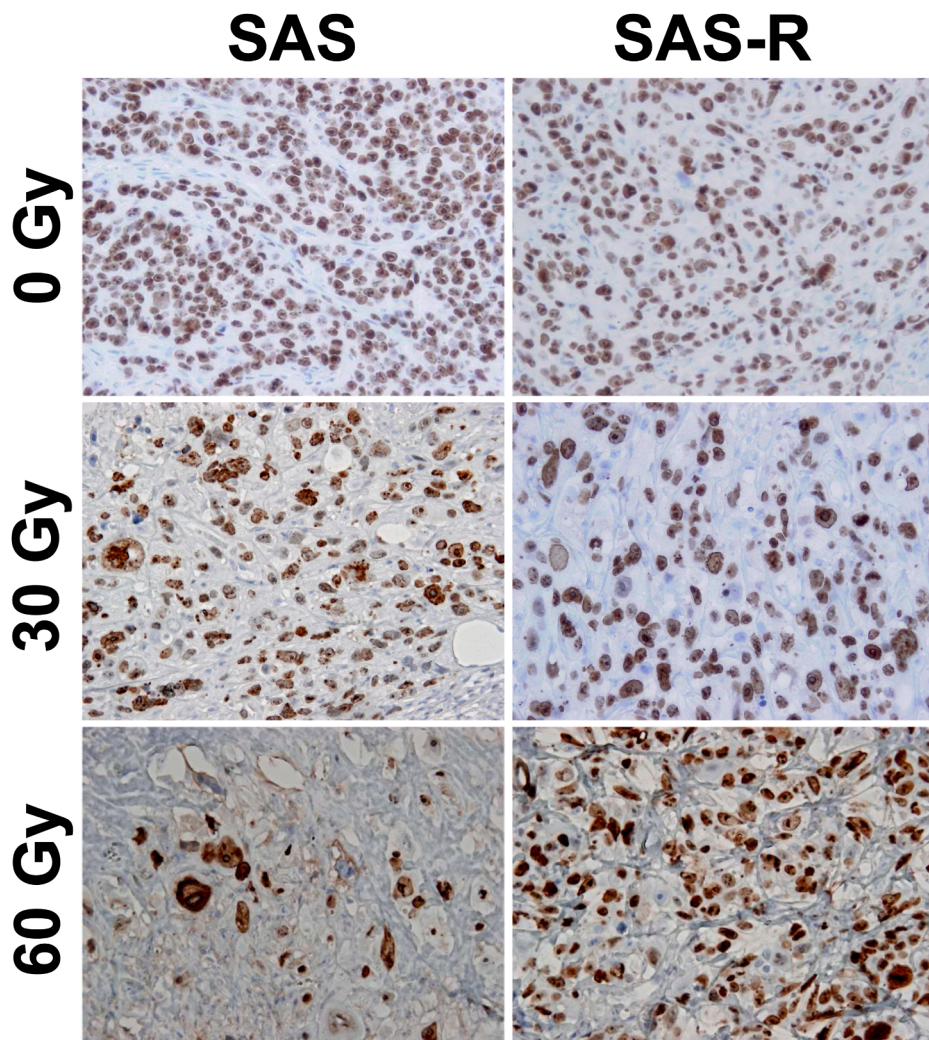


Figure 4 Determining the growth fraction of parental SAS and clinically relevant radioresistant SAS-R tumor cells by detecting Ki-67 positive cells. In SAS tumors, the number of dividing cells decreased as the radiation dose increased. However, no obvious decrease in dividing cells was observed in SAS-R tumor. The amount of connective tissue increased in SAS tumors as the radiation dose increased, but no obvious increases were observed in SAS-R tumors.

radiation exposure by TGF β signaling. Fibrosis has been reported to cause functional impairment in normal cells and to be related to radioresistance.³² In this study, we observed less fibrosis in CRR tumor indicating that CRR tumor were less damaged by irradiation. Our previous study also showed that fibrosis occurs more in the parent cells compared to CRR cells after irradiation.³³ These results suggest that SAS-R cells are resistant to fractionated irradiation *in vivo*.

The Ki-67 protein is present during all active phases of the cell cycle but is absent from resting G₀ cells. Thus, Ki-67 is an excellent marker for determining the growth fraction of a given cell population and is often used as a prognostic and diagnostic tool in cancer studies.³⁴ Our previous *in vitro* study showed that proliferation potency is maintained in CRR cells during exposure to 2 Gy/day of X-rays, whereas the proliferation potency is gradually lost in the parental cells.⁹ Ki-67 staining also showed that mitotic competent cells were reduced in SAS tumors. However, no significant reduction was detected in SAS-R tumors, suggesting that

stromal cells are not strongly involved in the radioresistance of tumor cells.

During autophagy, damaged or old cytoplasmic organelles and other cellular components are enclosed within double-membrane vesicles called autophagosomes. Autophagosomes fuse with lysosomes, where their contents are degraded and recycled. This process helps cells maintain homeostasis and respond to cellular stress, such as nutrient deprivation or oxidative stress. The process is usually cytoprotective, but autophagic cell death occurs when autophagy is excessive.³⁵ Autophagy after irradiation is highly context-dependent, contributing to treatment resistance or cell death, depending on the context.^{36,37} An electron microscopic analysis revealed that the cytoplasm of SAS cells was filled with autophagosomes, but only a small number of autophagosomes were observed in the cytoplasm of SAS-R cells. Furthermore, our previous study showed that the expression of LC3, an autophagy marker, increased when the SAS parent cells were irradiated. We also reported that CRR cells express less LC3 after

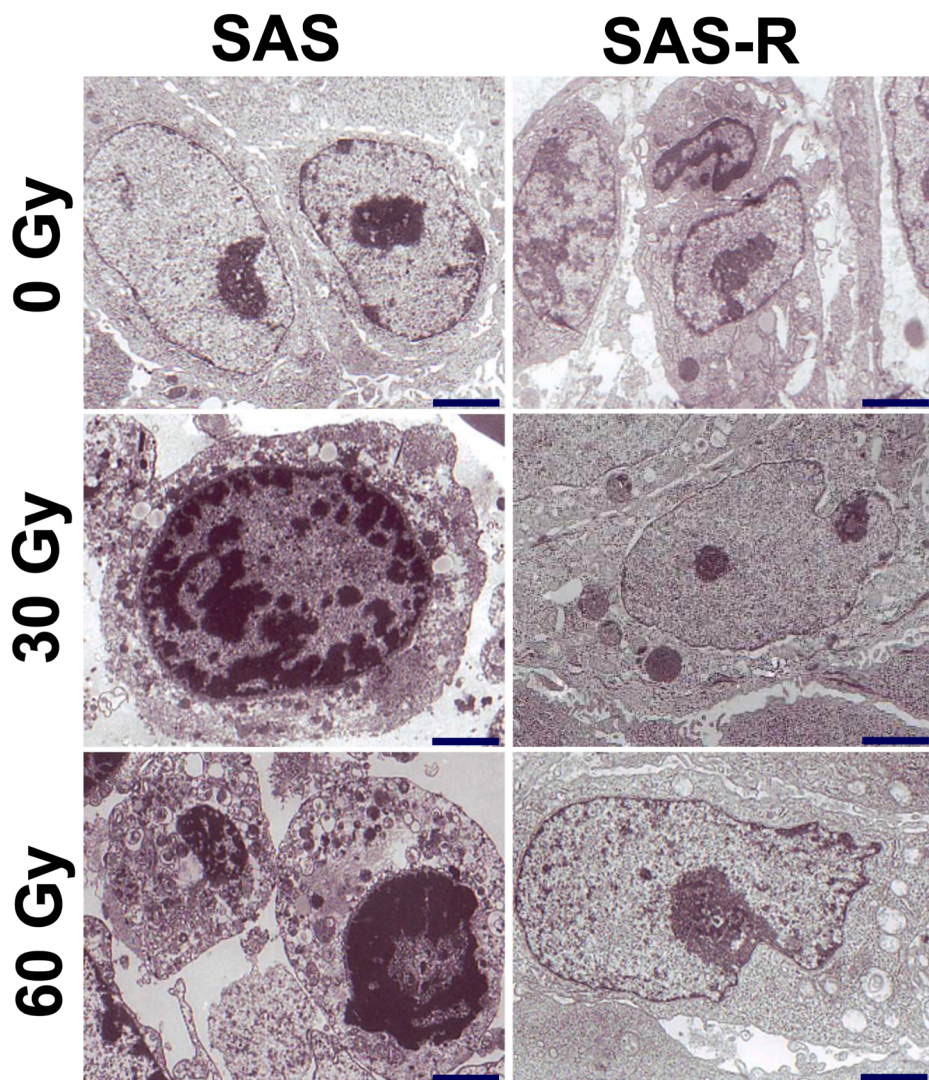


Figure 5 Electron microscopic analysis of parental SAS and clinically relevant radioresistant SAS-R tumor cells. The number of autophagosome-like structures increased in SAS tumor cells as the radiation dose increased, but no significant increase was observed in SAS-R tumor cells. In SAS-R tumor cells, a small number of spherical structures with double-layer membranes were observed with or without fractionated radiation. Scale Bar = 2 μ m.

irradiation compared to the parent cells.³⁸ These results suggest that autophagy induced by fractionated X-ray irradiation may be involved in cell death in SAS cells but may contribute to cell survival in SAS-R cells. However, further analysis is required to confirm these results. Moreover, immunodeficient mice lack a natural immune response. They therefore cannot reproduce the effects of the immune system on the microenvironment, such as the effects of T cells on cancer cells or phagocytosis by macrophages. Therefore, when we apply to clinical practice, it is necessary to consider the possibility that the behavior may not match the results of this study. This is a weakness of this model.

It has been reported that SAS parent cells cultured in the medium in which SAS-R was cultured formed more colonies after 6 Gy irradiation compared with untreated SAS parent cells, indicating that SAS-R cells can affect surrounding cells via the culture medium.³⁹ Therefore, tumor cells may act on the surrounding stromal cells to constitute an

environment conducive to their survival. If the cancer cells act on the surrounding stromal cells, then the cancer cells themselves that define the radioresistance of the tumor. This study indicates that cancer cells, not the surrounding stromal cells, define the radioresistance of the tumor.

Declaration of competing interest

The authors have no conflicts of interest relevant to this article.

References

- Bray F, Laversanne M, Sung H, et al. Global cancer statistics 2022: GLOBOCAN estimates of incidence and mortality worldwide for 36 cancers in 185 countries. *CA Cancer J Clin* 2024;74: 229–63.

2. Delaney G, Jacob S, Barton M. Estimation of an optimal external beam radiotherapy utilization rate for head and neck carcinoma. *Cancer* 2005;103:2216–7.
3. Herrera FG, Bourhis J, Coukos G. Radiotherapy combination opportunities leveraging immunity for the next oncology practice. *CA Cancer J Clin* 2017;67:65–85.
4. McDermott N, Meunier A, Mooney B, et al. Fractionated radiation exposure amplifies the radioresistant nature of prostate cancer cells. *Sci Rep* 2016;6:34796.
5. Larionova I, Rakina M, Ivanyuk E, Trushchuk Y, Chernyshova A, Denisov E. Radiotherapy resistance: identifying universal biomarkers for various human cancers. *J Cancer Res Clin Oncol* 2022;148:1015–31.
6. Zhang H, Wang X, Ma Y, et al. Review of possible mechanisms of radiotherapy resistance in cervical cancer. *Front Oncol* 2023; 13:1164985.
7. Yu K, Chen B, Aran D, et al. Comprehensive transcriptomic analysis of cell lines as models of primary tumors across 22 tumor types. *Nat Commun* 2019;10:3574.
8. Kolnöhuz A, Ebrahimpour L, Yolchuyeva S, Manem VSK. Gene expression signature predicts radiation sensitivity in cell lines using the integral of dose-response curve. *BMC Cancer* 2024;24:2.
9. Kuwahara Y, Li L, Baba T, et al. Clinically relevant radioresistant cells efficiently repair DNA double-strand breaks induced by X-rays. *Cancer Sci* 2009;100:747–52.
10. McDermott N, Meunier A, Lynch TH, Hollywood D, Marignol L. Isogenic radiation resistant cell lines: development and validation strategies. *Int J Radiat Biol* 2014;90:115–26.
11. de Llobet LI, Baro M, Figueras A, et al. Development and characterization of an isogenic cell line with a radioresistant phenotype. *Clin Transl Oncol* 2013;15:189–97.
12. Todorovic V, Prevc A, Zakelj MN, et al. Mechanisms of different response to ionizing irradiation in isogenic head and neck cancer cell lines. *Radiat Oncol* 2019;14:214.
13. Petragnano F, Pietrantoni I, Camero S, et al. Clinically relevant radioresistant rhabdomyosarcoma cell lines: functional, molecular and immune-related characterization. *J Biomed Sci* 2020;27:90.
14. Chan SPY, Yeo CPX, Hong BH, et al. Combinatorial functionalomics identifies Hdac6-dependent molecular vulnerability of radioresistant head and neck cancer. *Exp Hematol Oncol* 2025; 14:5.
15. Cannon A, Maher SG, Lynam-Lennon N. Generation and characterization of an isogenic cell line model of radioresistant esophageal adenocarcinoma. *Methods Mol Biol* 2023;2645: 139–52.
16. Carlos-Reyes A, Muniz-Lino MA, Romero-Garcia S, Lopez-Camarillo C, Hernandez-de la Cruz ON. Biological adaptations of tumor cells to radiation therapy. *Front Oncol* 2021;11: 718636.
17. Galeaz C, Totis C, Bisio A. Radiation resistance: a matter of transcription factors. *Front Oncol* 2021;11:662840.
18. Krisnawan VE, Stanley JA, Schwarz JK, DeNardo DG. Tumor microenvironment as a regulator of radiation therapy: new insights into stromal-mediated radioresistance. *Cancers (Basel)* 2020;12:2916.
19. Hellevik T, Martinez-Zubiaurre I. Radiotherapy and the tumor stroma: the importance of dose and fractionation. *Front Oncol* 2014;4:1.
20. Budach W, Taghian A, Freeman J, Gioioso D, Suit HD. Impact of stromal sensitivity on radiation response of tumors. *J Natl Cancer Inst* 1993;85:988–93.
21. Gerweck LE, Vijayappa S, Kurimasa A, Ogawa K, Chen DJ. Tumor cell radiosensitivity is a major determinant of tumor response to radiation. *Cancer Res* 2006;66:8352–5.
22. Ogawa K, Boucher Y, Kashiwagi S, Fukumura D, Chen D, Gerweck LE. Influence of tumor cell and stroma sensitivity on tumor response to radiation. *Cancer Res* 2007;67:4016–21.
23. Lundin P, Pedersen F. Volume of pituitary macroadenomas: assessment by MRI. *J Comput Assist Tomogr* 1992;16:519–28.
24. Liu JB, Hu L, Yang Z, Sun YU, Hoffman RM, Yi Z. Aurora-a/Nf-Kb signaling is associated with radio-resistance in human lung adenocarcinoma. *Anticancer Res* 2019;39:5991–8.
25. Pan L, Wu Q, Wang Y, Ma S, Zhang S. Characterization and mechanisms of radioresistant lung squamous cell carcinoma cell lines. *Thorac Cancer* 2023;14:1239–50.
26. Zhang L, Xie B, Qiu Y, et al. Rab25-mediated EGFR recycling causes tumor acquired radioresistance. *iScience* 2023;23: 100997.
27. Xie C, Chen X, Chen Y, et al. Mutual communication between radiosensitive and radioresistant esophageal cancer cells modulates their radiosensitivity. *Cell Death Dis* 2023;14:846.
28. Kuwahara Y, Mori M, Oikawa T, et al. The modified high-density survival assay is the useful tool to predict the effectiveness of fractionated radiation exposure. *J Radiat Res* 2010;51:297–302.
29. Kuwahara Y, Mori M, Kitahara S, et al. Targeting of tumor endothelial cells combining 2 Gy/day of X-ray with Everolimus is the effective modality for overcoming clinically relevant radioresistant tumors. *Cancer Med* 2014;3:310–21.
30. Rene AA, Nardone RM. The effect of gamma radiation on cell enlargement and size distribution of strain L. *Current Mod Biol* 1968;2:207–14.
31. Punnanitintont A, Kannisto ED, Matsuzaki J, et al. Sublethal radiation affects antigen processing and presentation genes to enhance immunogenicity of cancer cells. *Int J Mol Sci* 2020;21: 2573.
32. Margadant C, Sonnenberg A. Integrin-TGF-beta crosstalk in fibrosis, cancer and wound healing. *EMBO Rep* 2010;11: 97–105.
33. Kuwahara Y, Roudkenar MH, Urushihara Y, et al. Clinically relevant radioresistant cell line: a simple model to understand cancer radioresistance. *Med Mol Morphol* 2017;50:195–204.
34. Scholzen T, Gerdes J. The Ki-67 protein: from the known and the unknown. *J Cell Physiol* 2000;182:311–22.
35. Kroemer G, Levine B. Autophagic cell death: the story of a misnomer. *Nat Rev Mol Cell Biol* 2008;9:1004–10.
36. Levy JMM, Towers CG, Thorburn A. Targeting autophagy in cancer. *Nat Rev Cancer* 2017;17:528–42.
37. Glück S, Guey B, Gulen MF, et al. Innate immune sensing of cytosolic chromatin fragments through cGAS promotes senescence. *Nat Cell Biol* 2017;19:1061–70.
38. Kuwahara Y, Oikawa T, Ochiai Y, et al. Enhancement of autophagy is a potential modality for tumors refractory to radiotherapy. *Cell Death Dis* 2011;2:e177.
39. Yamana K, Inoue J, Yoshida R, et al. Extracellular vesicles derived from radioresistant oral squamous cell carcinoma cells contribute to the acquisition of radioresistance via the miR-503-3p-BAK axis. *J Extracell Vesicles* 2021;14:e12169.